Asymmetries in the discrimination of motion direction around the visual field

Rania Ezzo
Department of Psychology, New York University, New York, NY, USA
Department of Psychology, New York University Abu Dhabi, Abu Dhabi, UAE
NYUAD Research Institute, New York University Abu Dhabi, Abu Dhabi, UAE

Jonathan Winawer
Department of Psychology, New York University, New York, NY, USA
Center for Neural Science, New York University, New York, NY, USA

Marisa Carrasco
Department of Psychology, New York University, New York, NY, USA
Center for Neural Science, New York University, New York, NY, USA

Bas Rokers
Department of Psychology, New York University Abu Dhabi, Abu Dhabi, UAE
Center for Neural Science, New York University, New York, NY, USA
NYUAD Research Institute, New York University Abu Dhabi, Abu Dhabi, UAE

The discriminability of motion direction is asymmetric, with some motion directions that are better discriminated than others. For example, discrimination of directions near the cardinal axes (upward/downward/leftward/rightward) tends to be better than oblique directions. Here, we tested discriminability for multiple motion directions at multiple polar angle locations. We found three systematic asymmetries. First, we found a large cardinal advantage in a cartesian reference frame – better discriminability for motion near cardinal reference directions than oblique directions. Second, we found a moderate cardinal advantage in a polar reference frame – better discriminability for motion near radial (inward/outward) and tangential (clockwise/counterclockwise) reference directions than other directions. Third, we found a small advantage for discriminating motion near radial compared to tangential reference directions. The three advantages combine in an approximately linear manner, and together predict variation in motion discrimination as a function of both motion direction and location around the visual field. For example, best performance is found for radial motion on the horizontal and vertical meridians, as these directions encompass all three advantages, whereas poorest performance is found for oblique motion stimuli located on the horizontal and vertical meridians, as these directions encompass all three disadvantages. Our results constrain models of motion perception and suggest that reference frames at multiple stages of the visual processing hierarchy limit performance.

Introduction

Visual performance systematically depends on the visual field location of a stimulus. For example, it has been well-understood for over a century that visual performance is better for near than far eccentricities in humans (e.g. Wertheim, 1894; translated by Dunsky, 1980). This dependence of performance on visual field eccentricity relates to higher cone and retinal

Citation: Ezzo, R., Winawer, J., Carrasco, M., & Rokers, B. (2023). Asymmetries in the discrimination of motion direction around the visual field. *Journal of Vision*, *23*(3):19, 1–20, https://doi.org/10.1167/jov.23.3.19.

https://doi.org/10.1167/jov.23.3.19 Received November 23, 2022; published March 30, 2023 ISSN 1534-7362

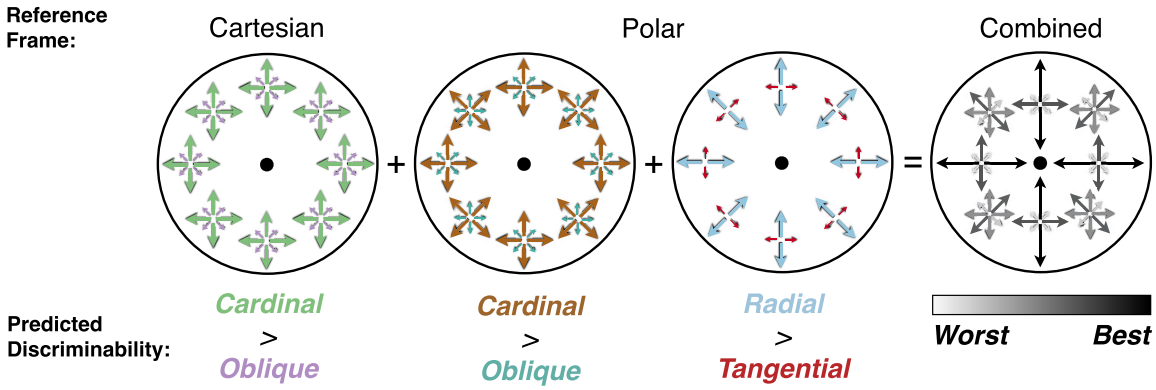

Figure 1. **Hypothetical asymmetries in sensitivity to motion direction in a cartesian and polar reference frame.** Arrow length indicates predicted sensitivity. Left to right: Cardinal (green) and oblique (purple) directions in a cartesian reference frame. The cardinal arrows are longer to depict a predicted cartesian cardinal advantage. Cardinal (brown) and oblique (teal) directions in a polar reference frame. The longer arrows depict a predicted polar cardinal advantage. Radial (blue) and tangential (red) directions in a polar reference frame. The longer blue arrows depict a predicted radial advantage. Combined advantages (gray) in both reference frames assuming an equal weight of cartesian cardinal, polar cardinal and radial advantages. The largest asymmetry effects are predicted along the primary meridians of the visual field (shown as difference in grayscale value). In principle, an unequal combination of these three factors might be observed.

ganglion cell density in the fovea (e.g. Weymouth, 1958; Curcio, Sloan, Kalina, & Hendrickson, 1990) and greater cortical magnification of the fovea (e.g. Cowey & Rolls, 1974; see review by Pointer, 1986). Visual performance for tasks involving acuity and contrast sensitivity also depends on polar angle (e.g. Carrasco, Talgar, & Cameron, 2001; Baldwin, Meese, & Baker, 2012; Barbot, Xue, & Carrasco, 2021), and these performance field asymmetries are paralleled by retinal and cortical factors (Kupers, Carrasco, & Winawer, 2019; Benson, Kupers, Barbot, Carrasco, & Winawer, 2021; Himmelberg et al., 2021; Himmelberg, Winawer, & Carrasco, 2022; Kupers, Benson, Carrasco, & Winawer, 2022).

Performance also varies systematically with visual features. Feature-based performance asymmetries, such as cardinal versus oblique orientations and motion directions, have been linked to differences in the number of neurons (Dragoi, Turcu, & Sur, 2001; Xu, Collins, Khaytin, Kaas, & Casagrande, 2006) and their tuning properties (Li, Peterson, & Freeman, 2003; Greenwood & Edwards, 2007). Charactering behavioral asymmetries can thus serve as a promising opportunity to connect behavior to the functional architecture of the visual system.

Stimulus features, such as orientation and motion direction, can be characterized with respect to *cartesian* or *polar* reference frames. Often the choice of reference frame is implicit. For example, many studies of optic flow adopt a polar reference frame because of the expanding and contracting flow fields produced by an observer moving through the environment. We investigated behavioral variation around the visual field while considering both cardinal and polar reference frames. We measured motion discriminability using local rather than global stimuli to (1) explore whether the directional asymmetries outlined below occur within spatially constrained regions of the visual field; and (2) probe whether behavioral asymmetries within different reference frames combine to explain behavior. Specifically, the set of polar angle locations tested allowed us to quantify the contribution of each directional asymmetry[1] outlined below by disentangling the effects from cartesian and polar reference frames.

Cartesian reference frame. Motion directions are often characterized and measured in a cartesian coordinate system. A well-known asymmetry in this framework is the "oblique effect for motion," which refers to better sensitivity for cardinal than oblique motion directions (Heeley & Buchanan-Smith, 1992; Gros, Blake, & Hiris, 1998; Matthews & Qian, 1999; Hupé & Rubin, 2004; Figure 1: Cartesian Cardinal > Oblique). Cardinality in the cartesian reference frame is invariant to stimulus position, and hence gaze direction (although not torsion of the eye). This cartesian cardinal advantage for motion likely results from greater exposure to these directions in natural environments. Based on an analysis of natural movies, local motion energy is greater and more narrowly distributed for cardinal than oblique motion directions (Dakin, Mareschal, & Bex, 2005).

Polar reference frame. Motion directions can also be characterized in a polar reference frame (i.e. radiating out from head or gaze position). Perceptual benefits

occur for radial and tangential motion directions compared to spiraling (Morrone, Burr, Di Pietro, & Stefanelli, 1999; Burr, Badcock, & Ross, 2001) or translating motion (Freeman & Harris, 1992; Lee & Lu, 2010). We grouped radial and tangential directions together as cardinal directions in the polar reference frame (Morrone et al., 1999) – polar cardinal – and considered directions that are neither tangential nor radial as oblique – polar oblique. In this polar reference frame, perceptual benefits occur for motion trajectories along a polar coordinate system's main axes, with gaze position as the origin (see Figure 1: Polar Cardinal > Oblique).

The polar cardinal advantage has been measured using global motion stimuli, as it is thought to involve flow fields corresponding to a motion processing stage after local motion signals are integrated (Burr et al., 2001; Lee & Lu, 2010). This asymmetry has been attributed to directional patterns resulting from optic flow patterns induced by self-motion (Morrone et al., 1999). It is an open question whether this directional asymmetry in the polar reference frame requires an actual flow field, or could also occur locally (i.e. for visual stimuli substantially smaller than the receptive field of an MST cell). Critically, the polar cardinal asymmetry has not been investigated for local motion signals.

A second motion direction asymmetry within the polar reference frame is greater sensitivity to radial than tangential motion directions (see Figure 1: Polar Radial > Tangential). Direction discrimination thresholds are lower when global dots move radially (Iordanova & van Grünau, 2001; Beardsley & Vaina, 2005; but see Kamitani & Tong, 2006); and response times for interocular suppression breakup are quicker when viewing dots moving radially than tangentially in separate visual field quadrants (Hong, 2015). Functional MRI (fMRI) BOLD activity is also greater for radial than tangential motion directions (Clifford, Mannion, & McDonald, 2009; Raemaekers, Lankheet, Moorman, Kourtzi, & Van Wezel, 2009). Similar to the polar cardinal advantage, it is unknown whether this radial benefit occurs for local stimuli and whether it varies with polar angle.

Relation between reference frames. Consistent with most visual features, asymmetries in motion sensitivity vary with eccentricity (Cormack, Blake, & Hiris, 1992; Coletta, Segu, & Tiana, 1993; Xu et al., 2006). It is unknown, however, whether and how the cartesian and polar cardinal advantages vary around the visual field for isoeccentric stimuli. If the directional advantages in the two reference frames combine, discriminability should be greatest for motion directions along the primary (horizontal and vertical) meridians of the visual field where their respective cardinal axes are aligned (see Figure 1: Combined). Were that the case, care should be taken to interpret variation in visual performance around the visual field as resulting from an asymmetry in one or the other reference frame in isolation. Analogous combinatorial benefits from multiple reference frames exist for static orientations (Sun et al., 2013; Shen, Tao, Zhang, Smith, & Chino, 2014), where the cartesian and polar advantages combine along the primary meridians. This has not been addressed in the motion domain because motion discrimination asymmetries have been measured with motion stimuli located at too few polar angle locations (Raymond, 1994) or that span too large a range of polar angles (e.g. entire visual hemifields; Levine & McAnany, 2005). Moreover, motion direction asymmetries are often measured with stimuli centered at fixation (e.g. Heeley & Buchanan-Smith 1992; Gros et al., 1998; Hupé & Rubin 2004; Meng & Qian, 2005; Greenwood & Edwards 2007).

Goals and motivation. The directional asymmetries outlined above have been investigated in separate experiments. A comprehensive approach quantifying the contribution of each of these asymmetries to overall direction discriminability around the visual field has been lacking. Measuring discriminability for several motion directions at several polar angles improves the current understanding of these asymmetries, and reveals the relative contribution of each of these effects as well as their potential interaction.

In summary, the goals of this study were as follows:

(1) To assess whether perceptual asymmetries for motion occur locally in both cartesian and polar reference frames.
(2) To test whether these asymmetries vary around the visual field (i.e. with polar angle).
(3) To provide a quantitative summary for how these asymmetries combine and together predict behavior.
(4) To compare the magnitude of these asymmetries using the same experimental protocol and observers.

The results have provided behaviorally relevant constraints for models of motion processing and inform future investigation about at which neural processing stages the asymmetries may arise.

Methods

Participants

Eight observers, with normal or corrected-to-normal vision, performed 2AFC motion direction discrimination tasks. Informed consent was obtained for each observer under New York University's Institutional Review Board, and observers were compensated for their time. The sample included seven

women and one man with an age range of 24 to 32 years old; one author was included (S01). All observers were right-handed. Six out of eight observers completed the full experiment. The remaining two observers only completed sessions for radial and tangential test directions and were only included in analyses directly comparing these conditions to prevent confounding effects of location.

Equipment and apparatus

Stimuli were presented on a 33.0 cm × 24.8 cm CRT monitor, with a refresh rate of 60 Hz and a resolution of 1152 × 864 pixels. The monitor was positioned 60 cm from the chinrest, providing a resolution of approximately 37 pixels per degree. A matte black circular aperture (radius = 10.9 degrees radius) was physically placed on the monitor to prevent potential effects from monitor edges/corners. The practice and experimental sessions described below were performed in a dark room. We used the Eyelink 1000 Plus Desktop Mount eyetracker (SR Research Ltd., Ontario, Canada) to enforce fixation throughout the stimulus period and to record gaze position throughout the experiment.

Visual stimuli

The experiment was programmed using MATLAB (MathWorks, Natick, MA, USA) and Psychtoolbox (Brainard, 1997; Kleiner, Brainard, & Pelli, 2007). Stimuli were presented in one of eight isoeccentric visual field locations: 7 degrees eccentricity and polar angles from 0 to 315 degrees in steps of 45 degrees. In each location, motion discrimination was performed relative to one of eight standard directions: 0, 45, 90, 135, 180, 225, 270, and 315 degrees.

The motion stimuli were Gabors, gratings drifting underneath stationary Gaussian envelopes. The sine wave gratings had a spatial frequency of 1 cpd and drifted at 8 cycles/s (hence 8 degrees/second). This speed was chosen for three reasons: (1) it is within the range of speeds that humans are perceptually sensitive to (Cooper, van Ginkel, & Rokers, 2016); (2) it is well-suited for designs probing local motion sensitivity without producing display artifacts/aliasing; and (3) asymmetries for motion occur around this speed and lessen in magnitude for slower speeds (Ball & Sekuler, 1987; Giaschi, Zwicker, Young, & Bjornson, 2007). We chose a relatively mid-to-low spatial frequency of 1 cpd to mitigate any strong perceptual effects from orientation throughout the task, while maintaining enough stimulus variation inside the small stimulus aperture. The Gaussian mask had a standard deviation of 0.43 degrees. The Gaussian masks were truncated at three standard deviations from their centers (a diameter of approximately 2.5 degrees). The stimulus was set to 50% contrast relative to the gray background prior to applying the Gaussian mask.

Stimulus sequence

During each trial, observers fixated on a black dot at the center of the display. Each trial began with a fixation period of 1300 ms, followed by a 500 ms target interval with the drifting Gabor (Figure 2). After the stimulus offset, the central fixation changed from black to red, prompting the observer to respond. Response time was not limited and observers received feedback for correct (high frequency tone) and incorrect (low frequency tone) responses. Trials with fixation breaks (≥1.5 degrees from center) anytime from 300 ms before the stimulus onset until the stimulus offset were aborted and moved to the end of the session. Based on this criterion, the number of aborted trials was <10% of the total number of completed trials for all but one observer (for S07, it was about 20%). The trial design and feedback were the same for both the main experiment and practice sessions.

Procedure

Observers reported whether the Gabor target's drift direction was clockwise or counterclockwise relative to an internal standard direction, which was verbally communicated to the observer and learned during a practice block prior to each session. During the practice block trials, the target drift direction deviated +/− 8 degrees from the standard; and observers practiced until they reached ceiling accuracy. During the full experiment, a method of constant stimuli was used to select one of 10 target drift directions for a given trial: 0.5, 1, 2, 4, and 8 degrees clockwise or counterclockwise from the internal standard direction. For a given session, the standard direction was fixed in the cartesian reference frame (e.g. upward, see Figure 2).

The full experiment, completed by six out of eight observers, consisted of 16 sessions, two for each of the eight standard directions. For each of the eight standard directions, one session tested polar angle locations of 0, 90, 180, and 270 degrees, and the other session tested polar angle locations of 45, 135, 225, and 315 degrees. The four polar angle locations were randomly ordered within a session. Sessions alternated between the two groups of locations and were ordered randomly with respect to direction. Sessions lasted approximately 1 hour each, with a total of 12,800 trials (20 repeats × 10 constant difficulty levels = 200 trials for each of the 64 unique direction-location conditions). We collected an additional 2240 trials (at all 8 locations of radial

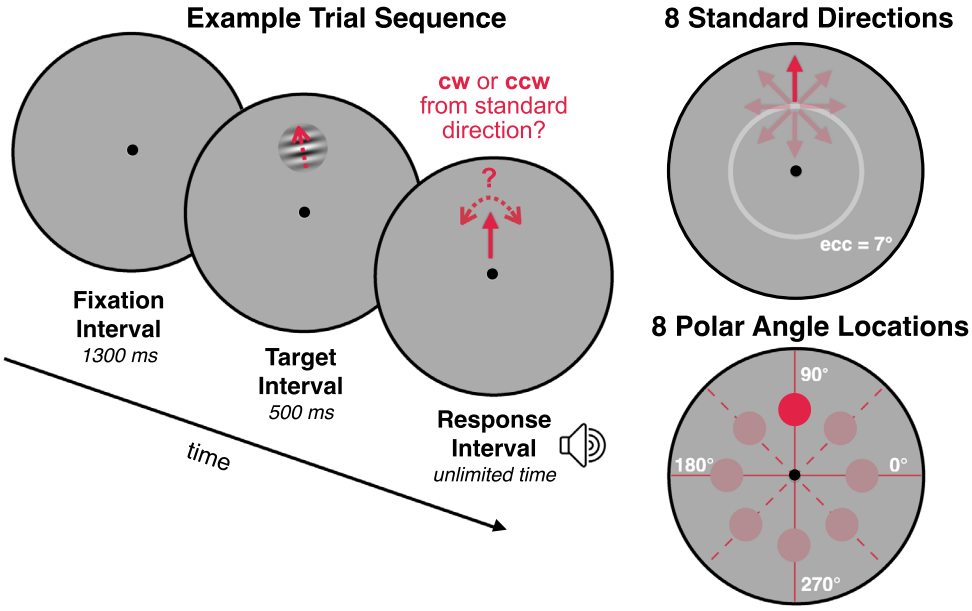

Figure 2. **Experimental design.** (Left) Observers performed a 2AFC motion direction discrimination task. After a fixation interval, the observer viewed a drifting Gabor pattern, and indicated whether the drift direction was clockwise or counterclockwise relative to the standard direction (here, upward), and then received auditory feedback. (Right) There were 64 conditions, crossing eight standard directions and eight polar angle locations: four locations were on the primary meridians (solid red lines) and four locations were off the primary meridians (dashed red lines) of the visual field. The standard direction was constant within an experimental session.

and tangential conditions) for observer S04 because a few of her psychometric fits had extreme bias and very low sensitivity. The remaining two observers (S07 and S08) completed only the sessions in which motion was radial or tangential, resulting in half the number of trials.

Analyses

Psychometric fitting

To estimate sensitivity and bias for each motion direction and each location (64 unique conditions in the full experiment), we fit cumulative gaussian distributions to the data:

$$\phi(x) = \lambda/2 + (1-\lambda)\left[\frac{1}{2}\left(1 + erf\left(\frac{x-\mu}{\sigma\sqrt{2}}\right)\right)\right]$$

Where x was the tilt angle relative to the standard direction, $\phi(x)$ was the % clockwise responses for each tilt angle, λ was the lapse rate, and erf(x) was the error function. The model was fit with two free parameters: μ was the bias, and σ was inversely related to sensitivity. Lapse rate was fixed to 0.01, an approximated rate of inaccurate key presses (Kingdom & Prins, 2010). After the fitting procedure, we ensured each psychometric function adequately captured the observer responses at each tilt value (minimum $R^2 = 0.739$). Performance metrics were then based on the parameter estimates of these psychometric fits, μ and σ.

For each psychometric fit, sensitivity was computed as $1/\sigma$, indicating the precision of an observer's responses. Sensitivity served as the primary measure of perceptual discriminability. Bias magnitude, or $|\mu|$ derived from the model, was the secondary measure. The magnitude of bias characterized the angular offset from the true direction (in degrees) at which the observer had equal clockwise/counterclockwise responses. This criterion captured the degree to which the psychometric function horizontally shifted away from the center; and bias values away from zero indicated the observer systematically reported the target direction as more clockwise/counterclockwise than the presented direction (see Figure 2).

Perceptual sensitivity and bias magnitude may be inversely related because perceptual uncertainty may lead observers to rely more on heuristics or external factors. Some evidence points to a systematic relation between the two metrics, where bias magnitude is close to zero when sensitivity is high (Loffler & Orbach, 2001; Wei & Stocker, 2017). However, there are mixed predictions for bias magnitudes for conditions with low sensitivity (Loffler & Orbach 2001; Wei & Stocker 2017). We explored this relation after we confirmed that signed bias values were distributed

around zero (Appendix S1; i.e. responses across conditions were not systematically more clockwise or counterclockwise).

Measuring behavioral asymmetries at each polar angle

We quantified three asymmetries, for which each asymmetry compared two direction conditions: (1) cartesian cardinal versus oblique, (2) polar cardinal versus oblique, and (3) radial versus tangential. For each observer, we averaged sensitivity estimates for each direction condition at each polar angle location. The same was done for bias magnitude. Confidence intervals (68%) for each direction condition were calculated using a bootstrapping procedure. In each iteration, the binary observer responses were randomly sampled with replacement for each direction and each location. Then the psychometric fitting procedure above was repeated (bootstraps = 1000 iterations). Within an observer's dataset, performance between conditions was considered significantly different if the confidence intervals did not overlap (i.e. if the means of the two distributions were separated by two standard deviations, one from each distribution).

For analysis across observers, repeated-measures analysis of variance (ANOVAs) tested for main effects per directional asymmetry and potential interactions with polar angle location. Post hoc analyses were conducted when the directional asymmetry and location demonstrated an interaction. The mean performance per direction condition across observers is shown in subsequent plots with ±1 SEM as error bars.

Summarizing results with linear mixed effects models

To quantify the relative impact of each asymmetry in motion discrimination, several linear mixed effects models were fit to the performance measures in a hierarchical manner. The hierarchy of the models (and subsequent nesting) was ordered from simplest to most complex (number of parameters). Two factors were considered to determine which asymmetry was considered more fundamental in our nesting procedure. First, a cartesian cardinal advantage has been measured locally (Dakin et al., 2005) whereas the polar advantages had not. Additionally, whereas advantages for polar cardinal (Morrone et al., 1999; Burr et al., 2001) and radial (Beardsley & Vaina 2005) have been measured for global motion, evidence for the latter is mixed (Kamitani & Tong 2006). Second, we also considered the results from the repeated-measures ANOVAs when outlining the nested hierarchy.

The model fitting procedure and the subsequent model comparison were done separately to predict sensitivity and bias magnitude measurements. For all models in the hierarchy, observer identity was modeled as a random effect and all other variables were included as fixed effects. Model parameters included: the weights for each fixed effect (β_n), the variance components for the random effect of observer ($\sigma^2{}_{b0}$), and an error term ($\sigma^2{}_{\varepsilon}$). These parameters were estimated using the maximum likelihood (ML) procedure using the *fitlme* function in MATLAB.

We report results from four models. The baseline model assumed directional isotropy for each individual observer. The model in the next level accounted for behavioral differences in cardinal versus oblique directions in the cartesian reference frame. In the third level, we added a fixed effect to account for differences in cardinal versus oblique directions in the polar reference frame. In the fourth level, we added a fixed effect for radial versus tangential directions. All models were otherwise identical. The fourth model included effects for all three asymmetries considered in this study, and was formulated as:

$$\begin{aligned} y_{im} &= \beta_0 + \beta_1(\textbf{cartesian\_cardinal\_vs\_oblique}_{im}) \\ &\quad + \beta_2(\textbf{polar\_cardinal\_vs\_oblique}_{im}) \\ &\quad + \beta_3(\textbf{radial\_vs\_tangential}_{im}) + b_{0m} + \varepsilon_{im}, \end{aligned}$$

where:

- y_{im} was the observation i within observer grouping variable m
  - $i = i^{th}$ observation (either the extracted sensitivity/bias magnitude values derived from the psychometric fits), e.g. $i = 1, 2, \ldots 64$
  - $m = m^{th}$ observer; e.g. $m = 1, 2, \ldots$ *n_observers*
- β_0 was the global intercept
- β_1, β_2, and β_3 were the weights derived for each motion direction asymmetry
  - **cartesian_cardinal_vs_oblique** was 1 for cart_cardinal or -1 for cart_oblique,
  - **polar_cardinal_vs_oblique** was 1 for pol_cardinal or -1 for pol_oblique
  - **radial_vs_tangential** was 1 for radial, -1 for tangential, 0 for neither
- b_{0m} was the random effect for level m of grouping variable *observer*, with a prior distribution $b_{0m} \sim \mathrm{N}(0, \sigma^2{}_{b0})$
- ε_{im} was the error term, with a prior distribution $\varepsilon_{im} \sim \mathrm{N}(0, \sigma^2{}_{\varepsilon})$

Notation convention from Scott, Shrout, and Weinberg (2013).

The Bayesian Information Criterion (BIC) was used to determine which model best accounted for the observed data; lower ΔBIC indicates a better fitting model (while penalizing for the cost of additional model parameters). We reported model results (e.g. model comparison scores and parameter estimates) which were fit to the six observers with full datasets. However, we tested all models using both the constrained sample

($n = 6$) as well as the entire sample ($n = 8$) and the best fitting model remained the same for both cases.

We additionally performed a leave-one-out cross validation (LOOCV) procedure as an alternative model comparison method with less implicit assumptions. Using the LOOCV method, we assessed how well each model could predict performance across the 64 unique conditions. In this procedure, we computed predictions for condition *i* (one of the unique 64 location-direction conditions) by iteratively fitting the linear mixed effects models to a training set (number of datapoints in the training set per iteration = (64 – 1) * *n_observers*). Then, the error was computed between the predicted values and the actual values in the test set (all data points across the observer grouping variable *m* for condition *i*).

Results

Advantage for cardinal motion directions in a cartesian reference frame

We tested motion discrimination for eight different motion directions at each visual field location. As described in the Methods section, we fit psychometric functions to obtain sensitivity and bias magnitude estimates (Figure 3A). We first grouped data by cartesian cardinal versus oblique directions for each observer, averaged across all visual field locations. Sensitivity was greater for cardinal than oblique directions ($F(1, 5) = 37.633$, $p = 0.002$; see Figure 3B). These results are consistent with the cartesian cardinal advantage for local motion stimuli (Dakin et al., 2005). There was a marginal interaction between this main effect and location ($F(7, 35) = 2.543$, $p = 0.032$). We then performed post hoc analyses to compare the effect at each location separately. There was a significant cartesian cardinal advantage at each of the on-meridional locations, 0 degrees ($p = 0.002$), 90 degrees ($p = 0.002$), 180 degrees ($p = 0.004$), and 270 degrees ($p = 0.010$). The cartesian cardinal advantage was marginal at the off-meridional locations: 45 degrees ($p = 0.028$), 135 degrees ($p = 0.061$), 225 degrees ($p = 0.023$), and 315 degrees ($p = 0.022$; see Figure 3C, Figure 4A).

We next evaluated the relation between sensitivity and bias magnitude across observers using Spearman's correlation analysis and there was a strong negative correlation between the two metrics, ($r(6) = -0.929$, $p = 0.002$; Figure 5). Consistent with this, bias magnitude was smaller for cardinal than oblique directions ($F(1, 5) = 21.415$, $p = 0.006$). Measurements of bias magnitude were influenced by a marginal interaction between the main effect and location ($F(7, 35) = 2.699$, $p = 0.024$). Additionally, the bias magnitudes modulated based on whether on or off primary meridians (see Appendix S2A). The modulating effect was due to a co-occurring polar cardinal advantage. This is because cartesian and polar cardinal benefits align at the primary meridians resulting in an amplified effect, whereas they are

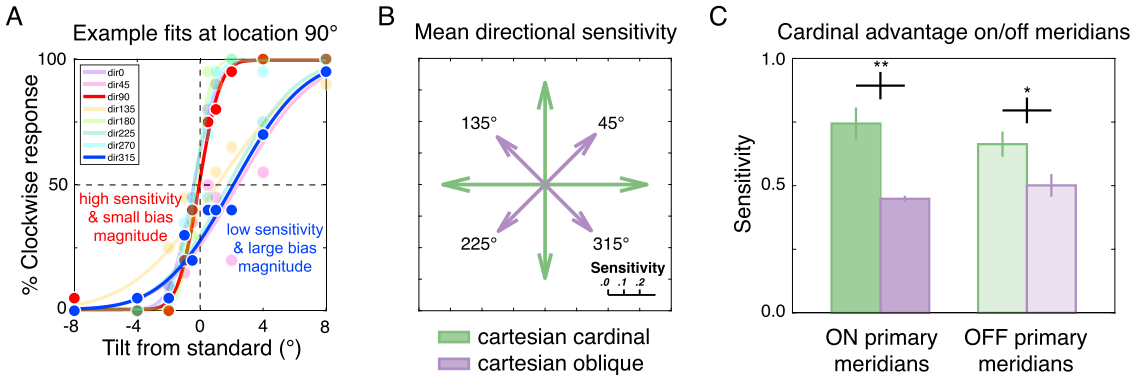

Figure 3. **Sensitivity estimates demonstrate a cartesian cardinal advantage.** (**A**) Example psychometric fits for S01 at location 90 degrees demonstrates high sensitivity and small bias magnitude (red curve/text) for upward compared to low sensitivity and high bias magnitude (blue curve/text) for upper leftward motion directions at this location. Each curve was estimated from 200 trials (20 trials/tilt angle). At this location, sensitivity to upwards directions = 0.97 (units: 1/degrees) and bias magnitude = 0.07 (units: degrees); sensitivity to lower rightwards directions = 0.53 and bias magnitude = 2.10. (**B**) Mean sensitivity (represented by arrow length) for each motion direction collapsed across all eight locations. Sensitivity was greater for cartesian cardinal than cartesian oblique directions. (**C**) Mean sensitivity to cartesian cardinal and cartesian oblique directions grouped based on whether the stimulus was located ON or OFF the primary meridians of the visual field. Grouping the data this way shows that the cartesian cardinal advantage was greater on than off the primary meridians.

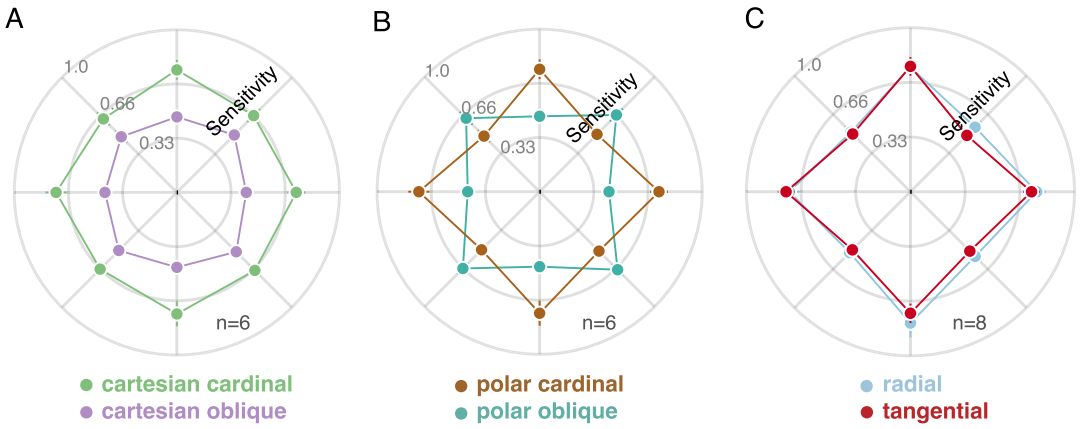

Figure 4. **Sensitivity to motion direction varies systematically around the visual field.** (**A**) Mean sensitivity for cardinal compared to oblique motion directions in cartesian reference frame. Each plotted point represents the mean performance for each condition across observers at eight polar angle locations. Each value prior to averaging was derived from four psychometric fits per condition for a given observer. Lines connect the dots. Error bars not visible were smaller than the plotting symbols. (**B**) Same data points as in **A** but re-grouped to compare mean sensitivity for polar cardinal compared to polar oblique directions at eight polar angle locations. (**C**) Mean sensitivity for radial compared to tangential directions at eight polar angle locations.

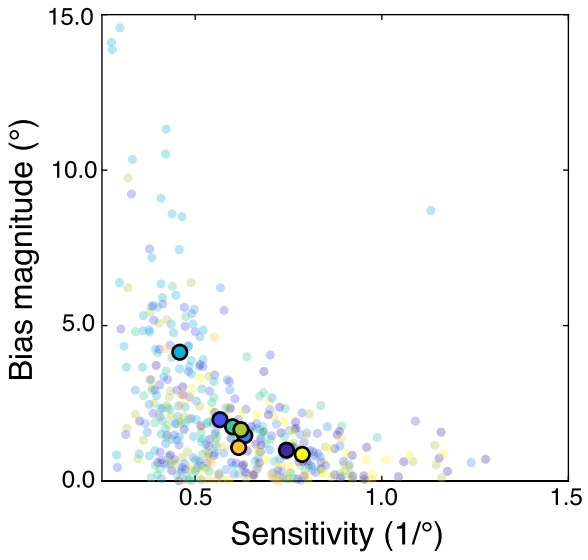

Figure 5. **Sensitivity negatively correlates with bias magnitude.** Opaque dots represent average sensitivity/bias magnitude estimates per observer. Translucent dots represent estimates derived from each psychometric fit. As sensitivity increased, bias magnitude decreased, demonstrating a negative correlation.

orthogonal off the primary meridians resulting in a dampened effect.[2] Overall, sensitivity and bias magnitudes were negatively correlated, but there was no systematic relation between sensitivity and (signed) bias direction.

Advantage for cardinal motion directions in a polar reference frame

The "cardinal axes of optic flow" are analogous to cardinality in the cartesian reference frame, except up-down-left-right are defined relative to fixation instead of in absolute terms. We re-grouped the data defining direction conditions as polar cardinal (radial or tangential) versus polar oblique (any other direction). Across locations, the difference in sensitivity did not reach statistical significance at the group level ($F(1, 5) = 3.355$, $p = 0.126$), but a significant interaction ($F(7, 35) = 28.561$, $p < 0.0001$) resulted from opposing effects on and off the primary meridians, confirmed by visual inspection (see Figure 4B: note the data points are identical but regrouped from Figure 4A). Bias magnitude was marginally smaller for polar cardinal than polar oblique ($F(1, 5) = 6.239$, $p = 0.055$), and was similarly driven by the locations along the primary meridians. The bias magnitudes (Appendix S2B) were inversely related to the sensitivity measures.

Advantage for radial motion directions

We assessed the possibility that the polar cardinal advantage was driven by radial directions specifically. On average, sensitivity was marginally greater and bias slightly smaller for radial compared to tangential directions when pooled across all locations ($F(1, 7) = 5.458$, $p = 0.052$; $F(1, 7) = 6.283$, $p = 0.041$; see Figure 4C). This suggests that observers could better

discriminate radial than tangential directions, but this effect was relatively small and did not account for the polar cardinal advantage.

Variability across observers

There are individual differences in both 2D (Pilz & Papadaki, 2019) and 3D (Fulvio, Ji, & Rokers, 2021) motion tasks, which are consistent with known individual variation for functional and structural properties of motion-selective cortical areas (Kolster et al., 2010). Performance differences in motion tasks have been linked to stronger surround suppression in the spatial domain (Tadin, 2015) and greater internal noise reduction in the temporal domain (Daniel & Dinstein, 2021). In our dataset, performance varied considerably across the eight observers: average sensitivity ranged nearly two-fold, from 0.44 to 0.77, units in 1 / degrees, and average bias magnitude ranged five-fold, from 0.83 to 4.12, units in degrees.

We first quantified the extent of the three asymmetries within each participant. For example, to quantify the extent of asymmetry in sensitivity in the cartesian reference frame, we subtracted average oblique sensitivity from average cardinal sensitivity. Based on the confidence intervals derived from the bootstrapping method described in the Methods section, we then determined how many observers demonstrated a significant asymmetry. Then, considering those with reliable asymmetries, we reported the ratio between the largest and smallest differences.

We evaluated the six observers who had full datasets only. Five out of these six had significantly greater sensitivity for cartesian cardinal compared to oblique directions. The extent of the cartesian cardinal asymmetry ranged by a factor of approximately 1.71 across these observers. The other observer's data (S04) trended in the same direction. The two observers with partial data also had a significant asymmetry. All six observers exhibited lower bias magnitudes for cardinal directions, but the effect was significant for only one observer (S06).

We quantified the difference in performance for locations at the primary meridians, where directions were cardinal versus oblique in both reference frames. All six observers had significantly greater sensitivity for cardinal directions (factor of approximately 6.47). Similarly, bias magnitude was lower for cardinal directions. This effect was significant only for three observers (factor of approximately 4.14) and trended in the same direction for the other three observers.

Last, we compared the performance between the conditions with best (radial direction along primary meridians) versus worst performance (oblique directions along primary meridians). This sensitivity difference was significant (factor of approximately 2.29) for all but one observer (S04 had a lower but consistent effect). Four out of six showed a corresponding significantly lower bias magnitude (factor of approximately 1.69). The remaining two observers had a lower but consistent effect. See Appendix S3 for individual plots, and see Appendix S4 for group plots that include subjects with partial data.

Directional asymmetries combine linearly

We established an advantage for cardinal motion directions in the cartesian reference frame and an advantage for cardinal and radial directions in the polar reference frame. We modeled performance across all visual field locations as a linear combination of these three asymmetries and estimated their relative contribution. Unlike the analysis above, which considered each asymmetry in isolation, here, we computed the magnitude of each asymmetry as a combined weighted sum. We show that behavior can be predicted by linear combination of these asymmetries, supporting the notion that separate underlying mechanisms may arise at different stages of the motion processing hierarchy.

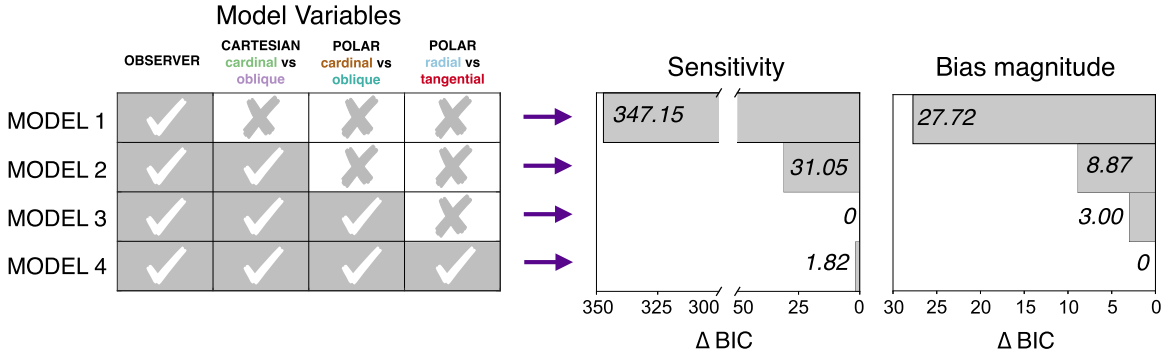

Figure 6. **Model comparison**. Several linear mixed effects models were tested. Observer identity was included as a random effect in all models. Directional asymmetries were fixed effects, with one additional effect added for each model. The Δ BIC scores were computed for each model for the sensitivity and bias magnitude measures.

	Sensitivity		Bias magnitude	
	Conditional R^2	Marginal R^2	Conditional R^2	Marginal R^2
Model 1	0.22	0.00	0.24	0.00
Model 2	0.63	0.41	0.28	0.04
Model 3	0.66	0.44	0.30	0.06
Model 4	0.66	0.45	0.31	0.07
	Sensitivity		Bias magnitude	
	Conditional F^2	Marginal F^2	Conditional F^2	Marginal F^2
Cartesian cardinal versus oblique	1.09	0.69	0.05	0.04
Polar cardinal versus oblique	0.10	0.06	0.03	0.02
Radial versus tangential	0.01	0.01	0.02	0.02

Table 1. **Goodness-of-fit (R^2) and Cohen's F^2 effect sizes**. Conditional R^2 (explained variance by the fixed and random effects) and marginal R^2 (explained variance by the fixed effects alone) values increased gradually from model 1 to model 4. Conditional F^2 and marginal F^2 indicate the effect sizes for each asymmetry. Based on sensitivity measures, the effect size was large for the cartesian cardinal asymmetry (small for bias magnitude), small for the polar cardinal asymmetry (also small for bias magnitude), and insubstantial for the radial tangential asymmetry (but reasonably small for bias magnitude).

Each linear mixed effects model we considered was fit first using the sensitivity estimates from the psychometric fits, then repeated for bias magnitude. As a baseline, in model 1, we assumed no directional asymmetry and accounted for random variation in mean performance across observers. This model performed the worst; it produced the largest BIC score. In model 2, we added a fixed effect for cartesian cardinal versus oblique directions, which greatly improved the model fit. In model 3, adding an additional fixed effect for polar cardinal versus oblique directions further improved the model fit. In model 4, we included an additional fixed effect for radial versus tangential directions. Both models 3 and 4 accounted for a substantial amount of systematic variability for both sensitivity and bias measures. These findings highlight a substantial impact of the polar reference frame on performance (Figure 6).

We computed goodness-of-fit values to provide information about the absolute model fit of the linear mixed models (see the Table 1). We included two measures: conditional R^2 (explained variance by the fixed and random effects) and marginal R^2 (explained variance by the fixed effects alone; Nakagawa & Schielzeth, 2013). We also computed the effect size of each asymmetry as Cohen's F^2 (see the Table 1), which are well-suited for evaluating effects from multiple regression models (Cohen, 1988).

Cross-validation approach confirms results from BIC model comparison

We additionally computed the explained variance for individual data points with a cross-validation procedure. We compared how well each model predicted performance for each observer at each of the unique 64 direction-location conditions. The results from this procedure confirmed that the three asymmetries accounted for a large amount of variation in sensitivity. As expected, the variance explained was very low for model 1, which assumed no systematic behavioral variation within observers ($R^2 = 0.20$). Model 2, which only included absolute cardinality as a fixed effect, predicted sensitivity values much better ($R^2 = 0.61$). Models 3 and 4 explained about the same amount of variance in sensitivity on the test set ($R^2 = 0.65$), demonstrating that accounting for asymmetries in the polar reference frame resulted in better behavior predictions than accounting for the cartesian asymmetry alone. The variance explained for individual datapoints was generally lower for bias magnitude (Appendix S6), suggesting other factors contributed to the variation for this performance metric. Model 4 provided a better account for bias magnitude than the other three models. The full model (model 4) was chosen to fit the behavioral data in the next section.

Effects of all three asymmetries generalize across observers

We plotted the estimated effect for each directional asymmetry derived from the linear mixed effects model. To assess whether model 4 generalized across observers, we derived 68% confidence intervals for each directional asymmetry by bootstrapping across observers 1000 times. These estimated effects were

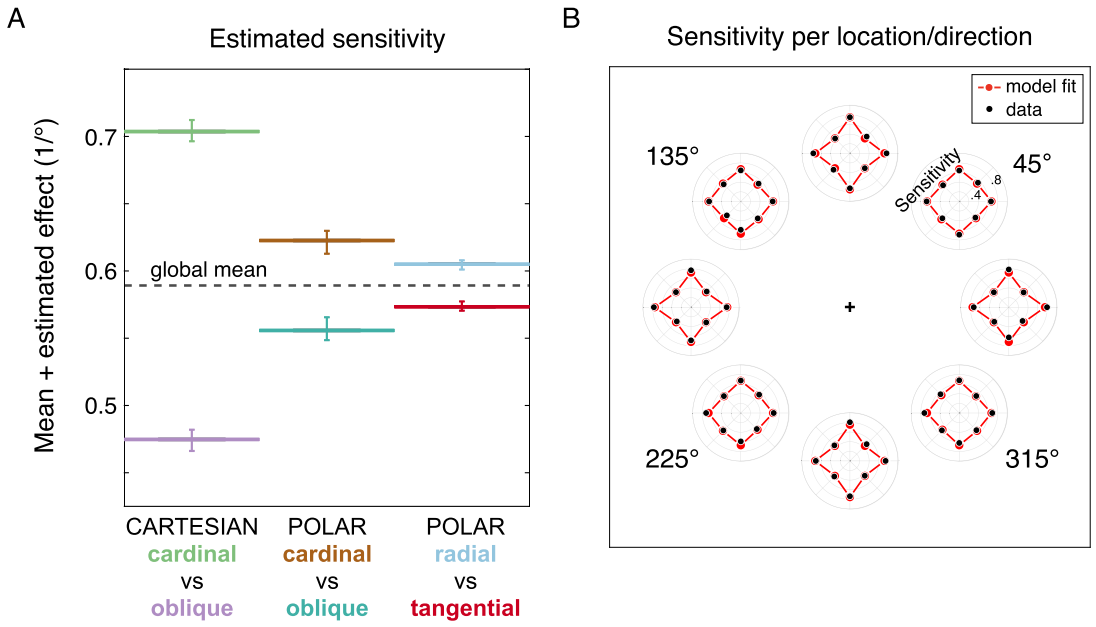

Figure 7. Parameter estimates and model fits demonstrate how directional asymmetries can explain behavioral variation in motion discrimination task. (**A**) Model 4 estimated weights for each asymmetry, relative to the global mean. Error bars represent 68% confidence intervals. (**B**) Directional asymmetries were greatest for locations at the primary meridians, the locations which have shared cardinal directions in cartesian/polar reference frames. Each polar plot shows mean performance for eight directions at a unique polar angle location. Lines represent the model fits reconstructed as $\beta_0 + \beta_1$ (cartesian_cardinal_vs_oblique$_{im}$) $+ \beta_2$ (polar_cardinal_vs_oblique$_{im}$) $+ \beta_3$ (radial_vs_tangential$_{im}$).

compared to assess the impact of each directional asymmetry irrespective of visual field location, and the confidence intervals demonstrate that sensitivity for the directions within each asymmetry not only differed from one another but also differed from the global mean (see Figure 7A; for bias magnitude see Appendix S5A). The cartesian cardinal advantage accounted for the largest amount of variance in performance, followed by the polar cardinal advantage, and last, there was a slight advantage for radial compared to tangential directions.

Effects of all three asymmetries capture the mean data

Model 4 parameter estimates were then compared to the data averaged across observers for each direction-location condition (see Figure 7B; for bias magnitude see Appendix S5B). The asymmetries were more pronounced on than off the primary meridians. Overall, parameter estimates from model 4 characterized the mean data remarkably well, indicating that a linear combination of the three asymmetries explained nearly all the variance in the group-average data ($R^2 = 0.93$).

Exploring other potential asymmetries of direction and location

We considered several alternative models, based on prior findings on motion discrimination. First, we considered whether the asymmetries in the polar reference frame can be better captured as a meridional advantage; this was important to test because directions in the polar reference frame covaried with location. To assess whether our results could be better explained by a combination of cartesian cardinal and meridional benefits, we tested an alternative model that included these two categorical factors as fixed effects and observer as a random effect ($\beta_0 + \beta_1$(cartesian_cardinal_vs_oblique$_{im}$) $+$ β_2(on_vs_off_primary_meridians$_{im}$) $+ b_{0m} + \varepsilon_{im}$). The model did not outperform model 4 either for sensitivity (ΔBIC $= 33.93$) or bias magnitude (ΔBIC $= 14.70$). This comparison demonstrates the data could not be better characterized based on co-occurring advantages for cartesian cardinal directions and meridional locations.

We then explored additional factors that might have accounted for the unexplained variation in our data. Including inward versus outward directions as an additional fixed effect to model 4 did not improve

model fits for either sensitivity (ΔBIC = 5.46) or bias magnitude (ΔBIC = 5.40). The presence and direction of this asymmetry was idiosyncratic both across observers and polar angle locations. See Appendix S3 and S7 plots for details.

Evidence for a lower visual field (LVF) advantage in human motion perception is mixed, see the Discussion section. Next, we separately tested an upper versus LVF asymmetry by adding it as a fixed parameter to model 4, which did not improve model fits for sensitivity (ΔBIC = 11.14) or bias magnitude (ΔBIC = 11.80).

In sum, the data could not be better explained by cartesian cardinal advantages with varying magnitudes at meridional locations. Additionally, neither outward versus inward nor the LVF versus the upper visual field (UVF) asymmetries accounted for the unexplained variance in behavior.

Discussion

We systematically tested local motion discrimination around the visual field and found that performance varied both with motion direction and visual field location. Discrimination was greatest for radial trajectories on the primary meridians of the visual field. These results were explained as a combination of asymmetries in motion direction discrimination in two different reference frames: A cardinal advantage in a cartesian coordinate system and cardinal/radial advantages in a polar coordinate system.

We characterized three local asymmetries (cartesian cardinal versus oblique, polar cardinal versus oblique, and radial versus tangential). Our findings confirmed that local discrimination of motion was better for cardinal than oblique directions in the cartesian reference frame (Dakin, et al., 2005). This study was the first to use local stimuli to measure discrimination advantages for cardinal over oblique directions and radial over tangential directions in the polar reference frame. Thus, all three asymmetries emerge at a processing stage preceding the integration of motion signals into global patterns.

We separately estimated variation in sensitivity in cartesian and polar coordinate systems. Performance was greatest for radial motion at the primary meridians, for example, when cartesian cardinal, polar cardinal, and radial directions aligned. Intermediate performance was observed when discriminating directions at locations off the primary meridians, which included a benefit of either cartesian or polar cardinality. Finally, performance was poorest for obliquely drifting motion at meridional locations.

These findings highlight that motion direction discrimination in the perifovea was asymmetric mainly with respect to direction within two reference frames rather than polar angle location. Directions in the polar reference frame varied with angular location but not along the cartesian reference frame. The relevance of polar angle on performance was parsimoniously explained by combining the two reference frames. These local asymmetries for motion discrimination combined in an approximately linear manner.

Relation between sensitivity and bias magnitude

We used a two-step approach to analyze the data (we fit psychometric functions to estimate parameters, then fit a linear mixed model). Estimating parameters separately for each of the 64 conditions was crucial because bias differed in sign across the motion directions. In other words, no systematic relation occurred between motion direction and signed bias (greater clockwise or counterclockwise responses); the overall mean of signed bias was normally distributed around zero (see Appendix S1). However, bias magnitude, like sensitivity, was systematically related to motion direction. Although these two metrics are mathematically independent in terms of the cumulative gaussian model, these estimated parameters were negatively correlated. We analyzed sensitivity and bias magnitude separately in subsequent model comparison procedures, to assess the deviation from zero bias regardless of sign, and to detect any important discrepancies between these two behavioral metrics as they relate to the asymmetries.

A possible reason for the inverse relation of sensitivity and bias magnitude is that when observers are less sensitive, they rely less on sensory evidence and more on one or more heuristics that do not prove helpful when discriminating motion in the range of directions tested. We conjecture heuristics can vary considerably across conditions and observers (e.g. axis attraction or repulsion, or response bias). Another reason for this inverse relation could be due to "low-level" sensory factors (e.g. integration mechanisms) that could result in different bias magnitudes based on direction (Loffler & Orbach, 2001; but see Wei & Stocker, 2017).

Although sensitivity and bias magnitude were inversely related, the radial versus tangential asymmetry was more pronounced for bias magnitude (see Appendix S5A) than sensitivity (see Figure 7A). We conjecture that whichever heuristics were adopted proved to be more helpful (or more detrimental) for radial (tangential) discrimination, possibility due to the simple geometrical relation between the internal standard direction and fixation position.

How generalizable are the three asymmetries?

Discrimination versus detection

Motion detection asymmetries for several motion directions and visual field locations have been reported. For example, detection sensitivity is greater for tangential compared to radial directions but only at the lowest speeds tested (<2 degrees/second at 6 degrees eccentricity; van de Grind, Koenderink, Van Doorn, Milders, & Voerman, 1993). In contrast, we found greater discrimination sensitivity for radial directions. We consider multiple factors that may explain these discrepant findings. First, behavior and underlying physiological mechanisms differ between motion detection and direction discrimination (Gros, et al., 1998; Bennett, Sekuler, & Sekular, 2007). Second, these directional asymmetries only occurred when observers were detecting displacements of small, slow-moving pixels. The authors suggested that these behavioral measures are linked to acuity (van de Grind, et al., 1993; also see Scobey & van Kan, 1991).

Speed

Separate mechanisms in the motion system process fast and slow speeds (Edwards, Badcock, & Smith, 1998; Giaschi, et al., 2007), and the cartesian cardinal asymmetry is absent below (<2 degrees/second; see experiment 3 in Ball & Sekuler, 1987). Asymmetries in the polar reference frame are also speed dependent; a tangential advantage occurs at very low speeds, but trends toward a radial advantage as speed increases (van de Grind, et al. 1993). This speed dependency would make the results from van de Grind, et al. (1993) and ours consistent. The asymmetries we reported are based on a stimulus drifting at 8 degrees/second; and we suspect these asymmetries more likely arise in cortical areas that are motion-selective.

Spatial frequency

We believe the three asymmetries we reported would generalize to other spatial frequencies. We avoided using a stimulus with a high spatial frequency to prevent observers from using orientation as a cue (because orientation and drift direction are orthogonal for drifting gratings).

Alternatives to gratings

Prior studies have reported the cartesian cardinal versus oblique asymmetry using a variety of stimuli, including random dot kinematograms (RDKs; Ball & Sekuler, 1987; Gros, et al., 1998; Meng & Qian, 2005) and drifting plaids (Heeley & Buchanan-Smith, 1992; Hupé & Rubin, 2004). Both polar asymmetries occur with global random-dot patterns (Freeman & Harris, 1992; Morrone, et al., 1999; Burr, et al., 2001; Iordanova & Grünau, 2001; Beardsley & Vaina, 2005). We predict RDKs to yield the same asymmetries we report, but to potentially overestimate the radial versus tangential effect due to transient motion streaks (Geisler, 1999). We refute that radial motion advantages can be attributed to transient motion streaks (Hong, 2015) because radial advantages occur for the motion direction of drifting gratings. See later discussion section "Could grating orientation explain our findings?"

Relation to previous studies: Other asymmetries

Directional asymmetry for inward versus outward motion

Both inward and outward directional advantages have been measured locally. However, there is mixed evidence for an outward (Georgeson & Harris, 1978; Ball & Sekuler, 1980) and inward (Edwards & Badcock, 1993; Raymond, 1994; Giaschi, et al., 2007) directional advantage. We found no evidence for either an inward or an outward directional advantage. It is possible that the eccentricity of our stimulus (7 degrees) is not optimal to capture either effect. The advantage for inward motion directions decreases (Edwards & Badcock, 1993) and the advantage for outward motion directions increases with eccentricity (Ball & Sekuler, 1980).

Location-based asymmetry: Performance fields

Separate visual field location asymmetries, such as the horizontal-vertical anisotropy (HVA) and the vertical meridian asymmetry (VMA) are well-established phenomena for static tasks that depend on factors such as contrast sensitivity and acuity (e.g. Carrasco, et al., 2001; Himmelberg, Winawer, & Carrasco, 2020; Barbot, et al., 2021). For specific motion-related tasks involving acuity judgments (short-range displacements), performance is better along the horizontal than the vertical meridian (van de Grind, et al., 1993). We do not find evidence for these asymmetries for the motion discrimination task in this study. We believe both HVA and VMA can be measured using motion stimuli (see discussion in Fuller & Carrasco, 2009); however, performance fields are more likely to occur for motion tasks that depend on more acuity and contrast sensitivity and for stimuli with increased spatial frequency and eccentricity. The three directional asymmetries in this study, however, should be considered when testing for performance field effects with motion stimuli.

Location-based asymmetry: Hemifield differences

Based on findings in nonhuman primates one might expect a lower visual field advantage for motion processing. A greater proportion of motion sensitive neurons have receptive fields in the LVF than the UVF in macaque MT (Gattass & Gross, 1981; Van Essen, Newsome, & Maunsell, 1984; Maunsell & Van Essen, 1987; Brewer, Press, Logothetis, & Wandell, 2002) and V1 (Van Essen, Maunsell, & Bixby, 1981). Similarly, a human study suggests that cortical area corresponding to the LVF in putative hMT has slightly greater visual field coverage when evaluated qualitatively (Amano, et al., 2009). However, these results are mixed. In proposed human MT, both fMRI BOLD activity (Tootell, Reppas, Kwong, Malach, Born, et al., 1995) and cortical representation demonstrate a lack of such asymmetry (Kolster et al., 2010). Moreover, a study mapping directional columns in human MT using high resolution fMRI methods revealed a similar distribution of direction preferences in the two hemifields (Zimmermann, Goebel, De Martino, Van de Moortele, Feinberg, et al., 2011).

Although there is at best weak evidence for differences in neural coding between upper and lower stimuli in human cortex, upper versus lower behavioral asymmetries have been demonstrated in human psychophysical tasks involving motion. Most of these studies have used motion detection tasks (Raymond, 1994 Experiment 2; Levine & McAnany, 2005; Zito, Cazzoli, Müri, Mosimann, & Nef, 2016). Evidence for an LVF advantage during direction discrimination has been mixed. For direction discrimination, at a similar eccentricity used in our study, the LVF advantage occurs in the presence but not in the absence of moving distractors (Rezec & Dobkins, 2004). This is consistent with our target-only protocol and findings. However, at further eccentricities (16-24 degrees), an LVF advantage occurs when discriminating radial motion in the absence of distractors (Edwards & Badcock, 1993), which is consistent with the greater amount of outwardly tuned neurons in the macaque LVF at large eccentricities (Albright, 1989). Overall, evidence for an LVF advantage in humans has been inconclusive. In the present study, we tested several directions and polar angle locations and found no systematic lower visual hemifield advantage across observers (neither for averaged directions nor for radial directions).

Alternative explanations

Could grating orientation explain our findings?

When the edges of a drifting grating are occluded by a circular aperture, the drift direction is perceived as orthogonal to the grating orientation (the aperture problem; Wallach, 1935). Because the drift direction can be deduced by the grating orientation alone, one may ask whether orientation asymmetries explain our results. We believe this is not the case for several reasons. First, radial orientation advantages have been shown behaviorally using static oriented gratings (Sasaki et al., 2006). A reliance on orientation would predict a benefit for tangential motion. However, we found a radial benefit with drifting gratings. Thus, the benefit for radial orientations may attenuate but cannot explain our results. Second, some have raised the possibility that the radial directional advantage may be an indirect consequence of a radial orientation advantage (Clifford et al., 2009; Hong, 2015). Here, our rationale behind using drifting gratings was partly to avoid transient orientation percepts (Geisler, 1999), as mentioned above, and to open the possibility for future studies to compare the magnitude of these asymmetries with drifting plaids. Third, some argue that both orientation and direction effects are driven by later cortical processing stages (i.e. in brain regions that are not orientation selective; Clifford et al., 2009; Raemaekers et al., 2009). Whereas this would produce a relationship between the radial asymmetry for orientation and direction, this does not imply that the direction asymmetry is derived from the orientation asymmetry.

Unlike the radial benefits for orientation and motion direction, which might counteract one another, the cardinal benefits in these two domains potentially work together. We believe that the cardinal advantage in our results is primarily based on motion direction for the following reasons. First, the cartesian cardinal direction advantage does not depend on orientation (Buchanan-Smith & Heeley, 1993; Hupé & Rubin, 2004). Second, the cardinal orientation/direction benefits are likely independent. Perceptual learning improvements in discriminating oblique orientation do not lead to improvements in discriminating oblique motion directions (Matthews, Liu, Geesaman, & Qian, 1999). Third, the participants seem to rely more on motion direction than the grating orientation, demonstrated by the advantage for radial drift despite the tangential orientation of the grating. It is likely this strategy did not change based on condition. Overall, the potential impact of orientation effects on the direction asymmetries would be small and that, given the overall pattern of results, the cardinal direction advantage cannot be explained by orientation.

Although the directional asymmetries in this study cannot be reduced to or explained by the orientation of the gratings, we recognize that motion perception is an estimation process that cannot be separated from non-directional features like position (Kwon, Tadin, & Knill, 2015) and motion axis orientation, even for stimuli with distributed spatiotemporal frequencies (Moon, Tadin, & Kwon, 2022). Because motion perception involves a hierarchical estimation

process, such features (e.g. axis orientation) are integral components for discriminating motion direction generally. We highlight that motion perception is not independent from such factors; nonetheless, the asymmetries result from motion-related mechanisms and generalize to other motion discrimination tasks.

Do our findings depend on the internal standard direction or learning?

Motion asymmetries are known to occur regardless of whether the observer uses an explicit standard direction or maintains an internal standard direction during an experimental task (Blake, Cepeda, & Hiris, 1997). We used internal standard directions to collect many trials in less time. The auditory feedback reinforced the internal standard direction throughout the experiment and minimized potential differences in learning rate across conditions. Learning rates are similar across motion conditions (e.g. cardinal versus oblique) if feedback is present (Ball & Sekuler, 1987).

Additionally, given that learning during motion discrimination tasks is specific to the trained motion direction (Ball & Sekuler, 1987), learning would not transfer across sessions. However, we explored whether learning occurred within sessions (which each consisted of 800 trials in total: 200 trials for 4 locations). Observers' performance was slightly better in the second than the first half of the session. Overall, the internal standard direction was maintained implicitly and relatively stable (see Appendix S8).

Potential origins and possible neural correlates

The cartesian and polar coordinate systems used to capture the directional asymmetries demonstrate that information is perceived and encoded using disparate neural representations (Soechting & Flanders, 1992). Characterizing direction discrimination in these two reference frames achieves a parsimonious account of the asymmetries that can fully characterize performance around the visual field. These asymmetries may arise from asymmetric sensory encoding of specific directions in both cartesian and polar reference frames, and/or may result from observers exploiting an internal representation of space as a grid/polar-like structure.

Origin of cartesian asymmetries

The cartesian cardinal benefit occurs based on the perceived, rather than the physical, direction and/or orientation of the stimulus (Heeley & Buchanan-Smith, 1992; Meng & Qian, 2005). Although this suggests the asymmetry arises after component motion signals are combined (Heeley & Buchanan-Smith, 1992), the local nature of the cartesian cardinal advantage leaves open the possibility that the asymmetry arises as early as V1 (Dakin et al., 2005). Despite this possibility, the cartesian asymmetry presents downstream from the early visual cortex (Churchland, Gardner, Chou, Priebe, & Lisberger, 2003) including temporal areas (Vogels & Orban, 1994).

Origin of polar asymmetries

Directions in the cartesian reference frame are invariant to position, unlike in the polar reference frame where directions vary with polar angle. The notion that polar asymmetries emerge later in the visual processing hierarchy may stem from the idea that these asymmetries emerge from neurons selective to complex motion patterns. Alternatively, polar asymmetries may result from a correlation of preferred direction and receptive field position.

There is mixed evidence regarding where the advantages associated with the polar reference frame originate. The first possibility is that these asymmetries originate at the retinal level. Radial asymmetries in general have been associated with an overrepresentation of radially elongated dendritic fields in many species (Leventhal & Schall, 1983; Rodieck, Binmoeller, & Dineen, 1985); and the asymmetry may be amplified in the early visual cortex (Schall, Perry, & Leventhal, 1986). Although these morphological asymmetries in the retina are consistent with a radial orientation advantage (Leventhal & Schall, 1983; Rodieck et al., 1985; Schall et al., 1986), they are also linked to an advantage for radial motion (Trenholm, Johnson, Li, Smith, & Awatramani, 2011; Sabbah et al., 2017).

A second possibility is that the asymmetry arises at the cortical level. Greater representation of neurons tuned for radial or tangential orientations depends on the layer of the early visual cortex of the monkey (upper and lower layers, respectively; Bauer & Dow, 1989). Both layers project to monkey MT, and if similar in the human MT, this could explain a polar cardinal advantage. The small advantage we report for radial motion may result from slightly greater connectivity between lower layers of V1 and MT in the human; or could alternatively be explained by a greater amount of radially directed horizontal connections in the early visual cortex (Raemaekers et al., 2009).

A third possibility is in cortical areas beyond the primary visual cortex. Radial directions and their orthogonal components are overrepresented in MT (Albright, 1989), and there is a radial advantage in the parietal cortex (Steinmetz, Motter, Duffy, & Mountcastle, 1987). Furthermore, encoding

information in polar coordinates is implicated in higher-level cognitive maps (Yousif, Chen, & Scholl, 2020) and in computing heading during self-motion (Cavalleri, Sabatini, Solari, & Bisio, 2003).

Development of the asymmetries

In nonhuman primates, there is a predisposition for polar and cartesian asymmetries, which increase with development (Shen et al., 2014). Whether or not a biological predisposition for these asymmetries exists in humans, they likely arise and strengthen based on natural scene statistics. Asymmetries in the polar reference frame are thought to arise from frequent exposure to radial/tangential motion. Polar asymmetries have been linked to eye/hand coordination and reaching (Maunsell & Van Essen, 1987; Steinmetz et al., 1987) and to optic flow patterns during self or world motion (Scott, Lavender, McWhirt, & Powell, 1966; Georgeson & Harris, 1978; Burr et al., 2001). The cartesian cardinal advantage for motion may be related to the frequent exposure to cardinal contours in the environment (Coppola, Purves, McCoy, & Purves, 1998; Girshick, Landy, & Simoncelli, 2011) for moving observers. If these asymmetries indeed develop because of more frequent exposure to specific directions, this could result in differentially tuned neurons that process the environment more efficiently.

Conclusion

The current study investigated whether and how motion discrimination varies with direction. We tested for and quantified three direction asymmetries: (1) a large benefit for cartesian cardinal relative to oblique, (2) a moderate benefit for polar cardinal relative to oblique, and (3) a small benefit for radial relative to tangential motion directions. These three asymmetries combined linearly to predict motion discrimination around the visual field, where asymmetries were more pronounced at the horizontal and vertical meridians than at the intercardinal locations. These findings highlight the importance of considering both cartesian and polar reference frames in the motion domain. Overall, the magnitudes of each asymmetry serve as predictions for studies related to natural scene statistics and motivate neuroimaging studies to further understand where the asymmetries arise and propagate in the brain. This future research will make possible a biologically plausible and behaviorally relevant framework for process models of motion perception.

Keywords: visual motion, perceptual asymmetry, radial bias, oblique effect, optic flow, cartesian reference frame, polar reference frame

Acknowledgments

The authors thank Patrick Shrout for advising on the notation of the linear mixed effects model.

Funded by the Global PhD Fellowship, New York University Abu Dhabi to author Rania Ezzo, the US National Institute of Health (NIH) National Eye Institute R01-EY027401 to authors Marisa Carrasco and Jonathan Winawer, Abu Dhabi Precision Medicine Aspire Research Institute VRI20-10 to author Bas Rokers, and Tamkeen New York University Abu Dhabi Research Institute CG012 to author Bas Rokers.

Data availability: Data and code are available at https://osf.io/834bd/.

Commercial relationships: none.
Corresponding author: Bas Rokers.
Email: rokers@nyu.edu.
Address: A2.107 – Computational Research Building, New York University Abu Dhabi, PO Box 129188, Abu Dhabi, United Arab Emirates.

Footnotes

[1]Some authors have referred to the asymmetries we outlined as "anisotropies." Given that the term "anisotropy" generally refers to an inhomogeneity in any direction, we prefer to use "asymmetries" to highlight a comparison between two groups of directions (e.g. cartesian cardinal versus oblique).
[2]The two observers who were only tested with radial/tangential directions were not included in this analysis. However, the reported effects are also present when including them (see Appendix S4).

References

Albright, T. D. (1989). Centrifugal directional bias in the middle temporal visual area (MT) of the macaque. *Visual Neuroscience, 2*(2), 177–188.

Amano, K., Wandell, B. A., & Dumoulin, S. O. (2009). Visual field maps, population receptive field sizes, and visual field coverage in the human MT+ complex. *Journal of Neurophysiology, 102*(5), 2704–2718.

Baldwin, A. S., Meese, T. S., & Baker, D. H. (2012). The attenuation surface for contrast sensitivity has the form of a witch's hat within the central visual field. *Journal of Vision, 12*(11), 23.

Ball, K., & Sekuler, R. (1980). Human vision favors centrifugal motion. *Perception, 9*(3), 317–325.

Ball, K., & Sekuler, R. (1987). Direction-specific improvement in motion discrimination. *Vision Research. 27*(6), 953–965.

Barbot, A., Xue, S., & Carrasco, M. (2021). Asymmetries in visual acuity around the visual field. *Journal of Vision, 21*(1), 2.

Bauer, R., & Dow, B. M. (1989). Complementary global maps for orientation coding in upper and lower layers of the monkey's foveal striate cortex. *Experimental Brain Research, 76*(3), 503–509.

Beardsley, S. A., & Vaina, L. M. (2005). Psychophysical evidence for a radial motion bias in complex motion discrimination. *Vision Research, 45*(12), 1569–1586.

Bennett, P. J., Sekuler, R., & Sekuler, A. B. (2007). The effects of aging on motion detection and direction identification. *Vision Research, 47*(6), 799–809.

Benson, N. C., Kupers, E. R., Barbot, A., Carrasco, M., & Winawer, J. (2021). Cortical magnification in human visual cortex parallels task performance around the visual field. *Elife, 10*, e67685.

Blake, R., Cepeda, N. J., & Hiris, E. (1997). Memory for visual motion. *Journal of Experimental Psychology: Human Perception and Performance, 23*(2), 353.

Brainard, D. H. (1997). The psychophysics toolbox. *Spatial Vision, 10*(4), 433–436.

Brewer, A. A., Press, W. A., Logothetis, N. K., & Wandell, B. A. (2002). Visual areas in macaque cortex measured using functional magnetic resonance imaging. *Journal of Neuroscience, 22*(23), 10416–10426.

Buchanan-Smith, H. M., & Heeley, D. W. (1993). Anisotropic axes in orientation perception are not retinotopically mapped. *Perception, 22*(12), 1389–1402.

Burr, D. C., Badcock, D. R., & Ross, J. (2001). Cardinal axes for radial and circular motion, revealed by summation and by masking. *Vision Research, 41*(4), 473–481.

Carrasco, M., Talgar, C. P., & Cameron, E. L. (2001). Characterizing visual performance fields: Effects of transient covert attention, spatial frequency, eccentricity, task and set size. *Spatial Vision, 15*(1), 61.

Cavalleri, P., Sabatini, S. P., Solari, F., & Bisio, G. M. (2003). Centric-minded templates for self-motion perception. *Vision Research, 43*(13), 1473–1493.

Churchland, A. K., Gardner, J. L., Chou, I. H., Priebe, N. J., & Lisberger, S. G. (2003). Directional anisotropies reveal a functional segregation of visual motion processing for perception and action. *Neuron, 37*(6), 1001–1011.

Clifford, C. W., Mannion, D. J., & McDonald, J. S. (2009). Radial biases in the processing of motion and motion-defined contours by human visual cortex. *Journal of Neurophysiology, 102*(5), 2974–2981.

Cohen, J. (1988). Chapter 9. Multiple regression and correlation analysis. *Statistical power analysis for the behavioral sciences* (2nd ed., pp. 407–413). Mahwah, NJ: Lawrence Erlbaum Associates.

Coletta, N. J., Segu, P., & Tiana, C. L. (1993). An oblique effect in parafoveal motion perception. *Vision Research, 33*(18), 2747–2756.

Cooper, E. A., van Ginkel, M., & Rokers, B. (2016). Sensitivity and bias in the discrimination of two-dimensional and three-dimensional motion direction. *Journal of Vision, 16*(10), 5.

Coppola, D. M., Purves, H. R., McCoy, A. N., & Purves, D. (1998). The distribution of oriented contours in the real world. *Proceedings of the National Academy of Sciences, 95*(7), 4002–4006.

Cormack, R., Blake, R., & Hiris, E. (1992). Misdirected visual motion in the peripheral visual field. *Vision Research, 32*(1), 73–80.

Cowey, A., & Rolls, E. T. (1974). Human cortical magnification factor and its relation to visual acuity. *Experimental Brain Research, 21*(5), 447–454.

Curcio, C. A., Sloan, K. R., Kalina, R. E., & Hendrickson, A. E. (1990). Human photoreceptor topography. *Journal of Comparative Neurology, 292*(4), 497–523.

Dakin, S. C., Mareschal, I., & Bex, P. J. (2005). An oblique effect for local motion: Psychophysics and natural movie statistics. *Journal of Vision, 5*(10), 9.

Daniel, E., & Dinstein, I. (2021). Individual magnitudes of neural variability quenching are associated with motion perception abilities. *Journal of Neurophysiology, 125*(4), 1111–1120.

Dragoi, V., Turcu, C. M., & Sur, M. (2001). Stability of cortical responses and the statistics of natural scenes. *Neuron, 32*(6), 1181–1192.

Dunsky, I. L. (1980). Peripheral visual acuity. *American Journal of Optometry and Physiological Optics, 57*, 915–924.

Edwards, M., & Badcock, D. R. (1993). Asymmetries in the sensitivity to motion in depth: A centripetal bias. *Perception, 22*(9), 1013–1023.

Edwards, M., Badcock, D. R., & Smith, A. T. (1998). Independent speed-tuned global-motion systems. *Vision Research, 38*(11), 1573–1580.

Freeman, T. C., & Harris, M. G. (1992). Human sensitivity to expanding and rotating motion:

Effects of complementary masking and directional structure. *Vision Research, 32*(1), 81–87.

Fuller, S., & Carrasco, M. (2009). Perceptual consequences of visual performance fields: The case of the line motion illusion. *Journal of Vision, 9*(4), 13.

Fulvio, J. M., Ji, M., & Rokers, B. (2021). Variations in visual sensitivity predict motion sickness in virtual reality. *Entertainment Computing, 38*, 100423.

Gattass, R., & Gross, C. G. (1981). Visual topography of striate projection zone (MT) in posterior superior temporal sulcus of the macaque. *Journal of Neurophysiology, 46*(3), 621–638.

Geisler, W. S. (1999). Motion streaks provide a spatial code for motion direction. *Nature, 400*(6739), 65–69.

Georgeson, M. A., & Harris, M. G. (1978). Apparent foveofugal drift of counterphase gratings. *Perception, 7*(5), 527–536.

Giaschi, D., Zwicker, A., Young, S. A., & Bjornson, B. (2007). The role of cortical area V5/MT+ in speed-tuned directional anisotropies in global motion perception. *Vision Research, 47*(7), 887–898.

Girshick, A. R., Landy, M. S., & Simoncelli, E. P. (2011). Cardinal rules: Visual orientation perception reflects knowledge of environmental statistics. *Nature Neuroscience, 14*(7), 926–932.

Greenwood, J. A., & Edwards, M. (2007). An oblique effect for transparent-motion detection caused by variation in global-motion direction-tuning bandwidths. *Vision Research, 47*(11), 1411–1423.

van de Grind, W. A., Koenderink, J. J., Van Doorn, A. J., Milders, M. V., & Voerman, H. (1993). Inhomogeneity and anisotropies for motion detection in the monocular visual field of human observers. *Vision Research, 33*(8), 1089–1107.

Gros, B. L., Blake, R., & Hiris, E. (1998). Anisotropies in visual motion perception: A fresh look. *JOSA A, 15*(8), 2003–2011.

Heeley, D. W., & Buchanan-Smith, H. M. (1992). Directional acuity for drifting plaids. *Vision Research, 32*(1), 97–104.

Himmelberg, M. M., Kurzawski, J. W., Benson, N. C., Pelli, D. G., Carrasco, M., & Winawer, J. (2021). Cross-dataset reproducibility of human retinotopic maps. *Neuroimage, 244*, 118609.

Himmelberg, M. M., Winawer, J., & Carrasco, M. (2020). Stimulus-dependent contrast sensitivity asymmetries around the visual field. *Journal of Vision, 20*(9), 18.

Himmelberg, M. M., Winawer, J., & Carrasco, M. (2022). Linking individual differences in human primary visual cortex to contrast sensitivity around the visual field. *Nature Communications, 13*(1), 1–13.

Hong, S. W. (2015). Radial bias for orientation and direction of motion modulates access to visual awareness during continuous flash suppression. *Journal of Vision, 15*(1), 3.

Hupé, J. M., & Rubin, N. (2004). The oblique plaid effect. *Vision Research, 44*(5), 489–500.

Iordanova, M., & van Grünau, M. W. (2001). Asymmetrical masking between radial and parallel motion flow in transparent displays. *Progress in Brain Research, 134*, 333–352.

Kamitani, Y., & Tong, F. (2006). Decoding seen and attended motion directions from activity in the human visual cortex. *Current Biology, 16*(11), 1096–1102.

Kingdom, F. A. A., & Prins, N. (2010). *Psychophysics: A practical introduction*. New York, NY: Elsevier Academic Press.

Kleiner, M., Brainard, D., & Pelli, D. (2007). What's new in psychtoolbox-3? *Perception, 36*:ECVP Abstract Supplement.

Kolster, H., Peeters, R., & Orban, G. A. (2010). The retinotopic organization of the human middle temporal area MT/V5 and its cortical neighbors. *Journal of Neuroscience, 30*(29), 9801–9820.

Kupers, E. R., Benson, N. C., Carrasco, M., & Winawer, J. (2022). Asymmetries around the visual field: From retina to cortex to behavior. *PLoS Computational Biology, 18*(1), e1009771.

Kupers, E. R., Carrasco, M., & Winawer, J. (2019). Modeling visual performance differences 'around' the visual field: A computational observer approach. *PLoS Computational Biology, 15*(5), e1007063.

Kwon, O. S., Tadin, D., & Knill, D. C. (2015). Unifying account of visual motion and position perception. *Proceedings of the National Academy of Sciences, 112*(26), 8142–8147.

Lee, A. L., & Lu, H. (2010). A comparison of global motion perception using a multiple-aperture stimulus. *Journal of Vision, 10*(4), 9.

Leventhal, A. G., & Schall, J. D. (1983). Structural basis of orientation sensitivity of cat retinal ganglion cells. *Journal of Comparative Neurology, 220*(4), 465–475.

Levine, M. W., & McAnany, J. J. (2005). The relative capabilities of the upper and lower visual hemifields. *Vision Research, 45*(21), 2820–2830.

Li, B., Peterson, M. R., & Freeman, R. D. (2003). Oblique effect: A neural basis in the visual cortex. *Journal of Neurophysiology, 90*(1), 204–217.

Loffler, G., & Orbach, H. S. (2001). Anisotropy in judging the absolute direction of motion. *Vision Research, 41*(27), 3677–3692.

Matthews, N., Liu, Z., Geesaman, B. J., & Qian, N. (1999). Perceptual learning on orientation and direction discrimination. *Vision Research, 39*(22), 3692–3701.

Matthews, N., & Qian, N. (1999). Axis-of-motion affects direction discrimination, not speed discrimination. *Vision Research, 39*(13), 2205–2211.

Maunsell, J. H., & Van Essen, D. C. (1987). Topographic organization of the middle temporal visual area in the macaque monkey: Representational biases and the relationship to callosal connections and myeloarchitectonic boundaries. *Journal of Comparative Neurology, 266*(4), 535–555.

Meng, X., & Qian, N. (2005). The oblique effect depends on perceived, rather than physical, orientation and direction. *Vision Research, 45*(27), 3402–3413.

Moon, J., Tadin, D., & Kwon, O. S. (2022). A key role of orientation in the coding of visual motion direction. *Psychonomic Bulletin & Review*, 1–11.

Morrone, M. C., Burr, D. C., Di Pietro, S., & Stefanelli, M. A. (1999). Cardinal directions for visual optic flow. *Current Biology, 9*(14), 763–766.

Nakagawa, S., & Schielzeth, H. (2013). A general and simple method for obtaining R2 from generalized linear mixed-effects models. *Methods in Ecology and Evolution, 4*(2), 133–142.

Pilz, K. S., & Papadaki, D. (2019). An advantage for horizontal motion direction discrimination. *Vision Research, 158*, 164–172.

Pointer, J. S. (1986). The cortical magnification factor and photopic vision. *Biological Reviews, 61*(2), 97–119.

Raemaekers, M., Lankheet, M. J., Moorman, S., Kourtzi, Z., & Van Wezel, R. J. (2009). Directional anisotropy of motion responses in retinotopic cortex. *Human Brain Mapping, 30*(12), 3970–3980.

Raymond, J. E. (1994). Directional anisotropy of motion sensitivity across the visual field. *Vision Research, 34*(8), 1029–1037.

Rezec, A., & Dobkins, K. (2004). Attentional weighting: A possible account of visual field asymmetries in visual search? *Spatial Vision, 17*(4), 269–293.

Rodieck, R. W., Binmoeller, K. F., & Dineen, J. (1985). Parasol and midget ganglion cells of the human retina. *Journal of Comparative Neurology, 233*(1), 115–132.

Sabbah, S., Gemmer, J. A., Bhatia-Lin, A., Manoff, G., Castro, G., Siegel, J. K., . . . Berson, D. M. (2017). A retinal code for motion along the gravitational and body axes. *Nature, 546*(7659), 492–497.

Sasaki, Y., Rajimehr, R., Kim, B. W., Ekstrom, L. B., Vanduffel, W., & Tootell, R. B. (2006). The radial bias: A different slant on visual orientation sensitivity in human and nonhuman primates. *Neuron, 51*(5), 661–670.

Schall, J. D., Perry, V. H., & Leventhal, A. G. (1986). Retinal ganglion cell dendritic fields in old-world monkeys are oriented radially. *Brain Research, 368*(1), 18–23.

Scobey, R. P., & van Kan, P. L. (1991). A horizontal stripe of displacement sensitivity in the human visual field. *Vision Research, 31*(1), 99–109.

Scott, M. A., Shrout, P. E., & Weinberg, S. L. (2013). Multilevel model notation—Establishing the commonalities. *The Sage Handbook of Multilevel Modeling,* 21–38.

Scott, T. R., Lavender, A. D., McWhirt, R. A., & Powell, D. A. (1966). Directional asymmetry of motion after-effect. *Journal of Experimental Psychology, 71*(6), 806.

Shen, G., Tao, X., Zhang, B., Smith, E. L., & Chino, Y. M. (2014). Oblique effect in visual area 2 of macaque monkeys. *Journal of Vision, 14*(2), 3.

Soechting, J. F., & Flanders, M. (1992). Moving in three-dimensional space: Frames of reference, vectors, and coordinate systems. *Annual Review of Neuroscience, 15*(1), 167–191.

Steinmetz, M. A., Motter, B. C., Duffy, C. J., & Mountcastle, V. B. (1987). Functional properties of parietal visual neurons: Radial organization of directionalities within the visual field. *Journal of Neuroscience, 7*(1), 177–191.

Sun, P., Gardner, J. L., Costagli, M., Ueno, K., Waggoner, R. A., & Tanaka, K. et al. (2013). Demonstration of tuning to stimulus orientation in the human visual cortex: A high-resolution fMRI study with a novel continuous and periodic stimulation paradigm. *Cerebral Cortex, 23*(7), 1618–1629.

Tadin, D. (2015). Suppressive mechanisms in visual motion processing: From perception to intelligence. *Vision Research, 115*, 58–70.

Tootell, R., Reppas, J. B., Kwong, K. K., Malach, R., Born, R. T., Brady, T. J., . . . Belliveau, J. W. (1995). Functional analysis of human MT and related visual cortical areas using magnetic resonance imaging. *Journal of Neuroscience, 15*(4), 3215–3230.

Trenholm, S., Johnson, K., Li, X., Smith, R. G., & Awatramani, G. B. (2011). Parallel mechanisms encode direction in the retina. *Neuron, 71*(4), 683–694.

Van Essen, D. C., Maunsell, J. H. R., & Bixby, J. L. (1981). The middle temporal visual area in the macaque: Myeloarchitecture, connections, functional properties and topographic organization. *Journal of Comparative Neurology, 199*(3), 293–326.

Van Essen, D. C., Newsome, W. T., & Maunsell, J. H. (1984). The visual field representation in striate cortex of the macaque monkey: Asymmetries, anisotropies, and individual variability. *Vision Research, 24*(5), 429–448.

Vogels, R., & Orban, G. A. (1994). Activity of inferior temporal neurons during orientation discrimination with successively presented gratings. *Journal of Neurophysiology, 71*(4), 1428–1451.

Wallach, H. (1935). Über visuell wahrgenommene Bewegungsrichtung. *Psychologische Forschung, 20*, 325–380.

Wei, X. X., & Stocker, A. A. (2017). Lawful relation between perceptual bias and discriminability. *Proceedings of the National Academy of Sciences, 114*(38), 10244–10249.

Wertheim, T. (1894). Über die indirekte Sehschärfe. *Zeitschrift für Psychologie und Physiologie der Sinnesorgane, 7*, 172, 189.

Weymouth, F. W. (1958). Visual sensory units and the minimal angle of resolution. *American Journal of Ophthalmology, 46*(1 Pt 2), 102–113.

Xu, X., Collins, C. E., Khaytin, I., Kaas, J. H., & Casagrande, V. A. (2006). Unequal representation of cardinal vs. oblique orientations in the middle temporal visual area. *Proceedings of the National Academy of Sciences, 103*(46), 17490–17495.

Yousif, S. R., Chen, Y. C., & Scholl, B. J. (2020). Systematic angular biases in the representation of visual space. *Attention, Perception, & Psychophysics, 82*(6), 3124–3143.

Zimmermann, J., Goebel, R., De Martino, F., Van de Moortele, P. F., Feinberg, D., Adriany, G., … Yacoub, E. (2011). Mapping the organization of axis of motion selective features in human area MT using high-field fMRI. *PLoS One, 6*(12), e28716.

Zito, G. A., Cazzoli, D., Müri, R. M., Mosimann, U. P., & Nef, T. (2016). Behavioral differences in the upper and lower visual hemifields in shape and motion perception. *Frontiers in Behavioral Neuroscience, 10*, 128.